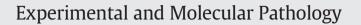
Contents lists available at ScienceDirect





journal homepage: www.elsevier.com/locate/yexmp



Copy number variants in clinical next-generation sequencing data can define the relationship between simultaneous tumors in an individual patient



Jennifer K. Sehn^{a,*}, Haley J. Abel^b, Eric J. Duncavage^a

^a Department of Pathology & Immunology, Washington University School of Medicine, St. Louis, MO 63110, USA
^b Department of Genetics, Washington University School of Medicine, St. Louis, MO 63110, USA

ARTICLE INFO

Article history: Received 21 May 2014 Accepted 29 May 2014 Available online 2 June 2014

Keywords: Deep sequencing Molecular diagnostics Copy number change Cancer Metastasis

ABSTRACT

Targeted next-generation sequencing (NGS) cancer panels have become a popular method for the identification of clinically predictive mutations in cancer. Such methods typically detect single nucleotide variants (SNVs) and small insertions/deletions (indels) in known cancer genes and can provide further information regarding diagnosis in challenging surgical pathology cases, as well as identify therapeutic targets and prognostically significant mutations. However, in addition to SNVs and indels, other mutation classes, including copy number variants (CNVs) and translocations, can be simultaneously detected from targeted NGS data. Here, as proof of methods, we present clinical data which demonstrate that targeted NGS panels can separate synchronous liver tumors based on CNV status, in the absence of distinct SNVs and indels. Such CNV-based analysis can be performed without additional cost using existing targeted cancer panel data and publically available software.

© 2014 Elsevier Inc. All rights reserved.

Introduction

The clinical application of next-generation sequencing (NGS) assays is growing, as targeted sequencing of panels of cancer genes can provide relevant information regarding diagnosis, prognosis, and treatment response in clinical samples of solid and hematolymphoid malignancies (Duncavage et al., 2012; Hadd et al., 2013; Hagemann et al., 2014; Nardi et al., 2013; Ross et al., 2013; Sehn et al., 2014; Spencer et al., 2013; Tothill et al., 2013; Tuononen et al., 2013). One real-world application of targeted NGS panels has been used to determine if synchronous or metachronous tumors occurring in the same or different sites represent the same 'tumor clone' or two unique tumors. In many cases the identification of two tumors versus a single tumor with multiple sites of involvement can have a significant impact on the choice of therapy. It is difficult, however, to establish the relationship between synchronous or metachronous tumors, particularly if the tumors share histologic features. In the past, loss of heterozygosity analysis was performed to establish the relationship between multiple tumors in these types of cases (Goldstein et al., 2005; Jiang et al., 2005; Jones et al., 2005; Li et al., 2008; Matias-Guiu et al., 2002; Nishimura et al., 2005; Shimizu et al., 2000; van der Sijp et al., 2002). Multiplex PCR assays interrogating known "hot spot" mutations also have been used to differentiate metastases from synchronous or metachronous primary tumors (Sequist et al., 2011; Su et al., 2011). More recently, targeted NGS assays for the detection of single nucleotide variants (SNVs) and small insertion/deletions (indels) in cancer-related genes have been applied to establish the relationship between metachronous tumors of the same histologic type occurring in an individual patient (Sehn et al., 2014).

Correct clinical and pathologic staging in patients with multiple malignant lesions is crucial to provide appropriate treatment and clinical management. For example, a patient with a 1.5 cm squamous cell carcinoma of the right lung and 1.5 cm squamous cell carcinoma of the left lung may have stage IV disease if one lesion is a metastasis from the other, or he/she may have two stage IA synchronous primary tumors, the treatment and prognosis of which is distinct (Goldstraw et al., 2007). Similarly, a patient with a history of squamous cell carcinoma in the right lung presenting with a new squamous cell carcinoma in the left lung following the treatment of the original lesion may have stage IV metastatic disease or stage IA metachronous primary tumors. Therefore, establishing the relationship between tumor types with differing morphologies is important for making informed treatment decisions.

The benefit of targeted NGS of cancer-related gene panels over traditional LOH or hotspot analysis in clinical cancer testing is directly related to the unique ability of NGS to simultaneously detect SNVs, indels, copy number variants (CNVs), and structural variants (SVs) including translocations and inversions. Appropriately designed clinical NGS assays can detect a full spectrum of clinically actionable variants across the

^{*} Corresponding author at: Department of Pathology and Immunology, Washington University School of Medicine, 660 S. Euclid Avenue, Campus Box 8118, St. Louis, MO 63110, USA.

E-mail address: jsehn@path.wustl.edu (J.K. Sehn).

entire coding region of cancer genes, without prior knowledge of what mutations are likely to be present in a given tumor sample. While the detection of SNVs and indels in clinical panels of cancer genes is well established, the feasibility and the usefulness of CNV detection in targeted NGS panels have not been as thoroughly evaluated (Cottrell et al., 2014; Pritchard et al., 2014). Here we describe the application of a clinical pipeline for CNV detection in targeted clinical NGS data, with emphasis on the contribution of CNV analysis in supporting the histologic interpretation of two separate tumors occurring simultaneously in the liver of an individual patient.

Materials and methods

Tissue samples

Ultrasound-guided needle core biopsies of multiple liver lesions were obtained for routine histologic assessment, leading to a diagnosis of simultaneous hepatocellular carcinoma (HCC) and neuroendocrine carcinoma (NEC). Formalin-fixed, paraffin-embedded tissue from each tumor was submitted for clinical NGS testing at Genomics and Pathology Services, Washington University in St. Louis (GPS@WUSTL). Pathologist review of a hematoxylin and eosin stained section from each tumor was used to guide tissue collection from the FFPE blocks. A board-certified pathologist marked areas of highest tumor cellularity and viability (estimated 90% and 95% in both tumors, respectively). Six 1-mm diameter tissue cores were collected from the HCC tissue block following the areas marked on the H&E guide slide; four cores were collected from the NEC block. The two tumors were submitted separately for NGS analysis, both for identification of predictive variants and for assessment of the relationship between the two tumors.

The Human Research Protection Office at Washington University has determined that case reports such as this do not constitute human subject research. This report was prepared in accordance with the Heath Insurance Portability and Accountability Act.

DNA extraction, capture, and sequencing

Targeted capture and next-generation sequencing of 40 cancerrelated genes (Comprehensive Cancer Gene Set version 2 assay, GPS@ WUSTL, St. Louis, MO) was performed on 1 µg of DNA from each of the two tumors, using a hybrid capture approach as previously described (Cottrell et al., 2014; Sehn et al., 2014). Briefly, genomic DNA was extracted from tissue cores and fragmented to an average length of ~200 bp using a Covaris ultrasonicator (Covaris, Woburn, MA). Fragmented DNA was end-repaired and ligated to sequencing adapters using the Agilent SureSelect library kit (SureSelect, Agilent Technologies, Santa Clara, CA). The following genes were targeted: ABL1, ALK, APC, ASXL1, ATM, BRAF, CEBPA, CTNNB1, DNMT3A, EGFR, ERBB2, ESR1, FGFR4, FLT3, IDH1, IDH2, JAK2, KIT, KMT2A (MLL), KRAS, MAP2K2, MAPK1, MET, MPL, MYC, MYD88, NOTCH1, NPM1, NRAS, PDGFRA, PIK3CA, PTEN, PTPN11, RB1, RET, RUNX1, TET2, TP53, VHL and WT1; additional genes (111) were targeted and used for CNV normalization/analysis, but not analyzed for SNVs and indels. Target enrichment was performed using custom solution-phase biotinylated cRNA capture baits (SureSelect, Agilent Technologies, Santa Clara, CA) complementary to all exons of the targeted genes with flanking regions (~800 kb). Specimen quality metrics were monitored throughout library preparation. Sequencing of the enriched DNA libraries was performed in multiplex on an Illumina HiSeq 2500 instrument using version 4 chemistry (Illumina, Inc., San Diego, CA) with the manufacturer's protocol for 101-bp paired-end reads.

Sequence analysis and SNV/indel interpretation were performed as previously described (Cottrell et al., 2014; Sehn et al., 2014). Briefly, sequence reads were aligned to the human reference genome (UCSC build hg19, NCBI build 37.2), followed by variant calling using the Genome Analysis Toolkit and Pindel (DePristo et al., 2011; Ye et al., 2009). Variants were compared to public databases to identify those likely to represent benign germline polymorphisms, namely variants present in >1% of normal individuals in dbSNP or the NHLBI Exome Variant Server (Exome Variant Server; Sherry et al., 2001). All other non-synonymous variants were further reviewed for accuracy and clinical significance by a Molecular Genetic Pathology fellow and a board-certified Molecular Genetic Pathologist.

Copy number variants (CNVs) were evaluated using the Copy Change Assessment Tool (CopyCAT) written by our laboratory for the evaluation of CNVs in small targeted panels. CopyCAT detects CNVs based on normalized log coverage ratios between samples and a pooled normal control (HapMap cell line DNA). Shifts in heterozygous variant allele frequencies away from the expected ratio of 0.5 are used to corroborate CNV calls.

Results

Pathologic examination

Gross examination of the right liver specimen showed an $8.2 \times 7.0 \times 6.4$ cm well-circumscribed, multilobulated, tan to yellow-green subcapsular mass. Two additional tan-pink nodules measuring 0.4 cm and 0.3 cm in maximum dimension also were identified, located more than 2 cm from the larger mass. The uninvolved liver parenchyma was grossly unremarkable.

Histologic examination of the large mass showed moderately differentiated hepatocellular carcinoma (Fig. 1A). Sections of the two smaller nodules showed sheets of highly atypical cells with nuclear hyperchromasia and so-called "salt and pepper" chromatin (Fig. 1B). These cells were reactive for CDX-2, synaptophysin, and chromogranin by immunohistochemistry (Fig. 1C). Ki-67 showed a proliferation index of 70–80% (Fig. 1D), diagnostic of a high-grade neuroendocrine carcinoma.

Clinically, the patient had no extrahepatic lesions or any history of additional cancers. The neuroendocrine carcinoma was a clinically unexpected finding, and its possible relationship to the hepatocellular carcinoma was a topic of discussion between the clinicians and pathologists.

Sequence metrics

A total of 21,965,302 reads were generated from the hepatocellular carcinoma sample, 6,401,241 (29%) of represented unique fragments that mapped to the targeted regions. Sequence coverage averaged 1354× over the capture region. Interestingly, exon-level coverage metrics failed quality control standards (>50× coverage for >95% of positions within each exon) for *RB1* exons 13–15 for the hepatocellular carcinoma sample. The first exon of several other genes also did not meet quality control metrics for coverage (Table 1).

The neuroendocrine carcinoma sample generated 23,481,628 reads, 6,488,401 (28%) of which were unique and on-target. Sequence coverage averaged $1371 \times$ over the capture region. While the first exon of several genes did not meet quality control standards for coverage (Table 1), *RB1* did show adequate coverage over all exons, including exons 13–15.

Sequence variants

No pathogenic SNV or small indel events were identified in either tumor. Two uncommon but previously reported germline polymorphisms (*ATM* p.A1309T and *NOTCH1* p.A1343V, rs149711770 and rs183156491, respectively) were seen in both cases. In contrast, the examination of the CNV plots showed distinct and non-overlapping profiles of larger deletions and duplications between the two tumor types. For example, the hepatocellular carcinoma sample showed copy number gains on chromosomes 5 and 7 as well as the *RB1* deletion

Download English Version:

https://daneshyari.com/en/article/5888334

Download Persian Version:

https://daneshyari.com/article/5888334

Daneshyari.com